

PHYSICOCHEMICAL AND PHOTOCATALYTIC PROPERTIES OF Fe⁺³-DOPED TiO₂ NANOTUBES FABRICATED VIA HYDROTHERMAL PROCESS

Jeffrey dG. Venezuela*

*Department of Mining, Metallurgical and Materials Engineering
College of Engineering, University of the Philippines*

ABSTRACT

Iron(III)-doped TiO₂ nanotubes were prepared by an impregnating-calcination method using the hydrothermally prepared titania nanotubes as precursors and Fe(NO₃)₃ as dopant. The samples were characterized by transmission electron microscope, x-ray diffraction and N₂ adsorption-desorption isotherm. The photocatalytic activity was evaluated by the photocatalytic degradation of methyl orange under visible-light irradiation. Surface structure analysis showed that the nanotube morphology was created at hydrothermal treatments of 120°C. The nanotube structure was preserved even after the doping-calcination step. X-ray diffractogram confirmed the presence of anatase and rutile in the processed titania. Surface area of the samples was observed to increase with increasing concentration of dopant. The 1.0% Fe⁺³-doped sample exhibited the highest photocatalytic activity. The high photocatalytic property of the Fe⁺³-doped TiO₂ powders could be attributed to the combined effects of Fe-doping, large specific surface area and small crystallite size.

1. INTRODUCTION

The use of titanium dioxide or titania (TiO₂) as a photocatalyst has drawn a lot of research and has led to the creation of innovative technologies with attractive application potentials. Some of these applications include self-cleaning and environmental pollution remediation; even antibacterial and antifungal applications [1-3]. This is mainly due to titania's ability to react with light and degrade a wide range of inorganic and organic compounds in both aqueous and gaseous phase [3-5]. This ability is described as photocatalytic property and allows titania to possess extremely strong oxidation capability. For example, organic matter, be it dyes, oils or even bacteria cells, breaks down into simple components when in contact with TiO₂ coated surfaces. In the Philippines, research on titania and its applications could have wide ranging implications and such research was undertaken in this study.

While titania is available in different forms, its most common commercial form is powder. Such consists of spherical shapes in the micrometer to submicrometer diameter range. With the recent trend going to nanostructure levels, studies have shown that titania can assume different nanoshapes. Nanospheres, nanotubes, nanosheets and nanorods are all possible with the proper processing technique. The advantage in going to nano-level sizes is enormous especially with respect to improving the photocatalytic properties of TiO₂. Since photocatalytic behaviour is surface dependent, the more than three-fold increase in surface area when the size goes into the nanometer range provides the necessary structure for this phenomenon to occur more intensely. Of special interest is the nanotube form of titania which possess a huge surface area to volume ratio and was proven to have outstanding photocatalytic power [6].

*Correspondence to: Department of Mining, Metallurgical and Materials Engineering, University of the Philippines, Diliman,, Quezon City, 1101, PHILIPPINES

Titania possesses three polymorphs though only two find commercial interest: anatase and rutile. Between the two, anatase exhibits the photocatalytic property. The band gap of anatase is 3.2 eV and the wavelength of light corresponding to this band gap is 380nm which is near-UV range. This means that the anatase's photocatalytic properties will only be triggered by exposure to UV light. However, UV light represents only a small fraction of visible light and this tends to limit titania's practical application. In view of making efficient use of solar energy, it is then important to develop titania with high activities under visible light radiation. A technique known as doping is employed to do such. This method requires adding an impurity ion into titania to lower the latter's band gap energy and allow absorption of lower energy radiation. Metals and its ions such as Sn, Fe, Cr and Co are found to be effective though C, S and N can work just as well [6-8]. Using Fe ions are attracting special attention after several researches proved it to be one of the most effective in degrading organic pollutants [7].

Many methods for titania synthesis have already been developed. Some of the techniques include the sol-gel process, chemical vapor deposition (CVD), and the hydrothermal process [2,9-11]. Compared with the other TiO_2 powders, TiO_2 synthesized by hydrothermal process has several advantages, such as being in the anatase crystalline form, having fine crystallite size with more uniform distribution and high-dispersion ability in various solvents, cheap and easy coating on different supporting material [12]. Calcination temperature above 450°C is usually required to form regular crystal structure in all of these processes, except for the hydrothermal process. Finally, the hydrothermal process was found to be successful in creating nanostructures, such as nanotube and nanorods of titania [11].

In this work, the hydrothermal process was employed in an attempt to fabricate titania nanotubes. Doping with Fe^{+3} ions was done to allow the nano-titania to be active even in visible light. After which, the physicochemical and photocatalytic properties of the fabricated titania was evaluated. The photocatalytic properties of the doped nanotubes were tested by the degradation of methyl orange under visible light.

2. METHODOLOGY

2.1 *Fabrication and Characterization of TiO_2 Nanotubes*

Commercial anatase titania powder were added to 30 mL of 10M NaOH in a Teflon beaker. The solution was mixed until the solid was well dissolved and then heated at different temperatures (100, 120, 130 and 140°C) for 24 hours. The solid obtained after heating was washed in 0.1 M HNO_3 and distilled water until the pH is brought to 7-8. The solids were dried at 100°C for an hour, and then ground using mortar and pestle. The powder was then kept in a dessicator to prevent moisture absorption.

The morphology of the samples fabricated at different temperatures was viewed using a JEOL transmission electron microscope. Since clearer images were observed from the viewing stage, a digital camera was used to capture these images directly. Only those which formed the nanotube structures will be used for further processing.

2.2 *Doping of Nanotubes with Fe^{+3}*

The processed titania powder having the nanotube form was then doped with Fe^{+3} ions using $\text{Fe}(\text{NO}_3)_3 \cdot 9\text{H}_2\text{O}$ as a the ferric ion source. Two concentrations, 1.0 wt% and 0.5 wt%, of ferric nitrate were prepared, and this is based on the atomic wt% of Fe compared to titania. Two hundred

milliliters of solutions were made. The nanotubes were added to the ferric salt solutions while making sure that the mixture's pH does not exceed 5. The mixture was stirred for 30 minutes with a magnetic stirrer, then soaked for 48 hours at room temperature. The color of the sample was observed to change from white to slight red-brown when doped.

2.3 Characterization of the Photocatalyst

2.3.1 Physicochemical Analysis

The fabricated material was subjected to different test to determine several properties. The chemical composition of the titania was characterized using an x-ray diffractometer with $\text{Cu}_{k\alpha}$ radiation in the region $\theta = 0$ to 80° . The average crystallite sized was estimated using the Scherrer's equation. The surface area was determined via nitrogen absorption using the Autosorb Quantachrome Instrument. For the BET analysis, powdered samples were degassed at 300°C for 1 hour prior to nitrogen adsorption measurements.

2.3.2 Photocatalytic Property Determination

The photocatalytic test involves degradation of an organic substance using the photocatalyst and visible light. Methyl orange was used as the representative organic pollutant. For each trial, one hundred (100) milliliters of 0.02 g/L (20 ppm) methyl orange solution was mixed with 0.2 grams of the doped catalyst and then exposed to a 150 W metal halide lamp. Initial feasibility runs were ran at exposure times of 1, 2, 4, 6 and 8 hrs. Results show that after 2 hours of exposure, very little methyl orange degradation was observed. It was thus decided to use the exposure time of 2 hours for the remaining tests.

The mixture was continuously stirred while under light exposure. After the exposure test, the solution was centrifuged and the decanted fluid tested for absorbance. A UV-VIS Spectrophotometer, set at 457 nm, was used to determine the amount of methyl orange remaining in the samples and the subsequent amount of degraded organic substance was then computed.

3. RESULTS AND DISCUSSION

3.1 Physicochemical Characteristics of Titania Nanotubes

3.1.1 Morphology of Titania Nanotubes

Transmission electron microscopy was used to reveal the structure created following the fabrication method. Since nanostructures are expected, very high magnifications are necessary for effective viewing. Figure 1 shows the titania structures created at different temperatures. In Figure 1a and 1b, elongated features were found in the sample. The denser outline as compared to the core further suggests that the elongated structure is hollow. Such a figure could then be imagined as straw-like or tube-like in feature. Indeed this figure confirms the successful creation of a nanotube as the diameter of the elongated structure falls in the ~ 100 nm range.

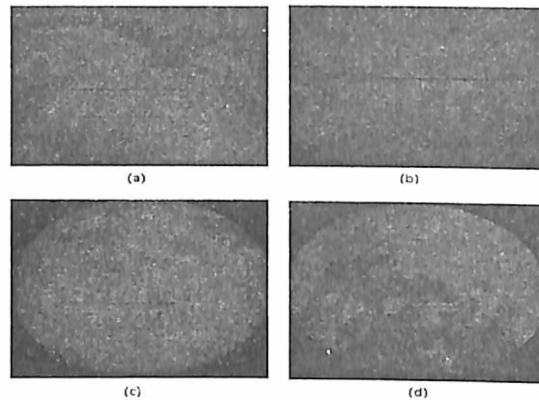


Figure 1. Micrographs of titania structures formed at (a) 100°C and (b) 120°C (taken 500kX) (c) 130°C and (d) 140°C (taken at 400kX)

The principle behind the formation of nanotubes during the hydrothermal process is the so-called scroll mechanism [13]. During alkali treatment, crystalline TiO_2 reacts with NaOH to form a highly disordered intermediate phase (containing Ti, O and Na) which later on recrystallizes into $\text{H}_2\text{Ti}_3\text{O}_7$ thin plates. But on the top surface, there is H-deficiency that leads to an asymmetrical environment for the surface $\text{Ti}_3\text{O}_{2.7}$ layer. This asymmetrical environment is the principal driving force of the cleavage of the single sheets of $\text{H}_2\text{Ti}_3\text{O}_7$ from the plates. Titania nanotubes were then formed by rolling up these single-layer TiO_2 sheets with a rolling-up vector of [001] forming single-walled nanotubes. Other sheets may also be attracted to surround these tubes forming the multi-walled nanotube.

The nanotube structures are observed to be formed only at a certain temperature range: 100 to 120°C. When the temperature exceeds 120°C, the structures begin to disintegrate into nano sheets (at 130°C) and eventually balls up (at 140°C). This transformation is but a thermodynamic response as the system aims to reduce the amount of surface area exposed as the temperature is increased. Furthermore, such observations are also similar to results reported in other researches [6].

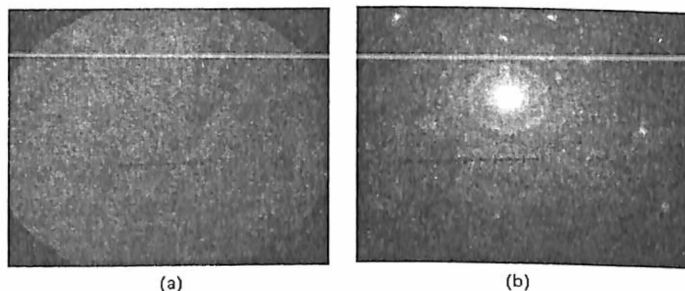


Figure 2. (a) Micrograph of Fe-doped titania structure (400kX) showing intact nanotube structure after calcinations at 400°C
(b) Electron diffraction of doped-titania confirms crystalline structure

The TEM micrograph of the Fe-doped titania sample (Figure 2a) reveals that the doping process, which involves calcination at 400°C, did not destroy the nanotube structure. Electron diffraction patterns of the nanotubes further confirms its crystallinity (Figure 2b). Titania nanotubes are found to be affected by temperature. These tubes are observed to collapse and form nanobelts and nanorods when heated at temperatures above 500°C [14]. Properties of the titania would subsequently be altered when such transformations occur.

3.1.2 X-ray Diffraction Analysis

The x-ray diffraction (XRD) patterns of undoped and Fe⁺³ doped titania samples are seen in Figures 3 and 4. Results confirm the presence of titania, in the anatase as well as in the rutile form, and calcium carbonate or calcite prior to doping. The latter is observed to be missing after doping. The presence of titania phases is as expected. The emergence of the anatase peaks coupled with the decline of rutile peaks after the doping-calcination suggests the transformation of rutile to anatase. Indeed such is the purpose of the calcination step and is similar to results published previously [7,14].

However, the presence of calcite is surprising. Indeed, the formation of this compound is impossibility if given that all the raw material used were correct. Confirmatory tests done on the raw titania powder used confirmed the presence of the white substance calcite (Figure 5). One can only surmise that calcite was added an extender for titania. On the other hand, the absence of calcite in the doped sample may then be explained. Calcite easily dissolves in weak acid. During the nanotube fabrication step where the powder was dissolved in HNO₃ acid, calcite dissolved together with titania. These two compounds precipitated during the heating step at 100°C as the acid evaporated. Indeed, calcite was detected by XRD. After doping, where the powder is again soaked in acid, the calcite again dissolved in the solution. The solution containing the calcite was eventually separated from the remaining solid and was discarded. As such, the undissolved solid contained only titania as seen in the XRD pattern (Figure 4).

Though immersed in Fe(NO₃)₃·9H₂O and discolored during the doping process, Fe₂O₃ or any other Fe_xTiO_y phases were not found in the XRD pattern of doped titania (Figure 4). This could be explained by the fact that the concentration of Fe-doping is so low that it cannot be detected by XRD. On the other hand, the radius of Ti⁺⁴ (0.68 Å) and Fe⁺³ (0.64 Å) are similar, therefore, the Fe⁺³ ions can also enter into the crystal structure of titania and locate at lattice sites of the titanium ion forming an iron-titanium solid solution [15]. This could then indicate successful incorporation of the ferric ions in titania. However, the ultimate confirmation for such an occurrence would be to use x-ray photoelectron spectroscopy (XPS).

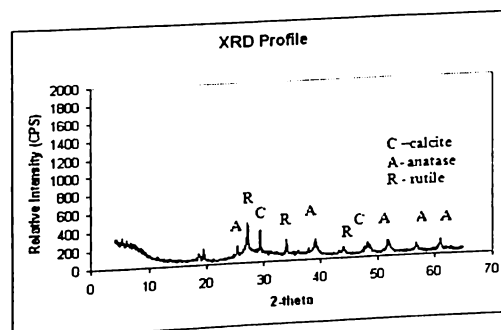


Figure 3. Diffraction pattern of undoped titania nanotubes formed at 100°C

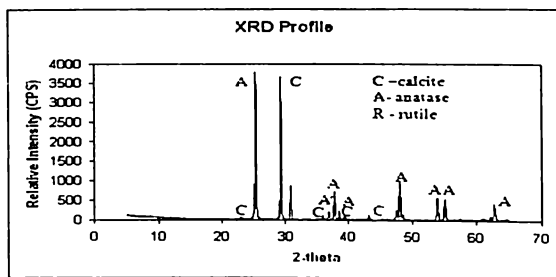


Figure 4. Diffraction pattern for Fe^{3+} -doped titania nanotubes formed at 100°C

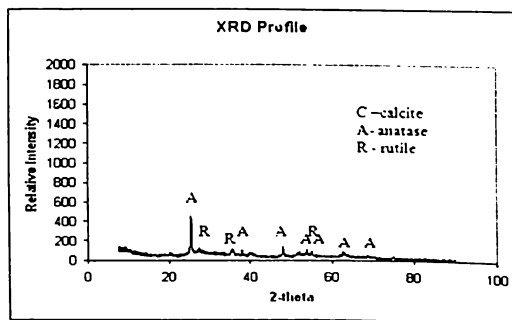


Figure 5. Diffraction pattern of as-received titania powder used as raw material

Table 1 shows the average crystallite size of the as-received titania, undoped and the Fe -doped nanotubes. Results simply confirm that the crystallite size refined when the titania powder is transformed to the nanotube. Indeed this is the objective of the hydrothermal treatment and points to the success of such a step. Between doped and undoped nanotubes, there is a slightly smaller crystal size in the doped nanotubes. This is also observed in other studies where doping [7,16] is involved, although the difference observed is indeed not significant. This is attributed to a more defined anatase crystal structure produced after the calcination treatment.

Titania Sample	Average Crystallite Size (nm)
As-received/untreated	81.48
Undoped nanotubes	58.41
0.5 wt% Fe^{+3} -doped nanotubes	52.57
1.0 wt% Fe^{+3} -doped nanotubes	49.38

3.1.3. Surface Area and Pore Distribution

The reactivity of TiO_2 photocatalysts is correlated with their surface area [17]. Heat treatment strongly influences the surface areas of the samples. Increasing calcination temperature would tend to decrease the crystal size, increase the surface area and increase the pore volume but only to a certain extent [18]. All samples were calcinated at 400°C , at temperatures higher than this ($\sim 600^\circ\text{C}$), high pore volume and surface area will not be preserved due to the collapsing of the tubes into rods and the formation of rutile [19].

Table 2 shows the total surface area and the pore profile of the iron doped and undoped samples. Surface area is observed to increase with increasing dopant addition. Such behaviour has also been observed in several studies [12,15]. After incorporation of ferric ions, surface charges may also have been induced because of the substitution of ferric ions into the titania lattice. This causes the nanotubes to repel each other, isolating each one and therefore revealing more surface.

Table 2. Surface area and pore distribution of titania samples

Titania Sample	Surface Area (m^2/g)	Pore Volume (cm^3/g)	Pore Size (nm)
1 wt% Fe^{3+} doped	228.44	5.212×10^{-2}	16.889
0.5 wt% Fe^{3+} doped	101.71	2.519×10^{-2}	18.747
Undoped	42.52	1.056×10^{-2}	18.434

The pore volume is also noted to increase as the nanotubes are doped. Compared to other studies [7], the obtained pore volume data is quite low. This is probably due to the isolation and separation of individual nanotubes as caused by the surface charges. In addition, the phase transformation of small anatase crystallites to rutile may also contribute to the increase in pore volume [20]. The pore size range for most of the samples were found to be in the range of 5-100 nm. The smaller pores (<10 nm) may correspond to the pores inside the nanotubes and the diameters of these pores are equal to the inner diameter of the nanotubes, while the larger pores (10–100 nm) can be attributed to the aggregation of the nanotubes [21]. Since the average pore area is relatively constant, at around 18 nm, it can be assumed that there are smaller pores than agglomerations in the nanotubes, especially for the 1 wt% Fe^{3+} doped titania, which showed a smaller average pore size. Finally, the observed pore size puts this material under the mesoporous type (2-100 nm) classification.

3.2 Photocatalytic Characteristics

Figure 6 shows the percent degradation of methyl orange under white light with doped and undoped titania. The exposure time used was 2 hours and the data show the mean of three trials. The photocatalytic property of the sample is judged from the amount of methyl orange degraded during light exposure. A high amount of degradation would indicate superior catalytic properties. Results point to a significant increase in photocatalytic activity under visible light of titania nanotubes with the addition of Fe^{3+} ions. Increasing dopant concentration also improved the same property. Such results agree with previous studies [7,15].

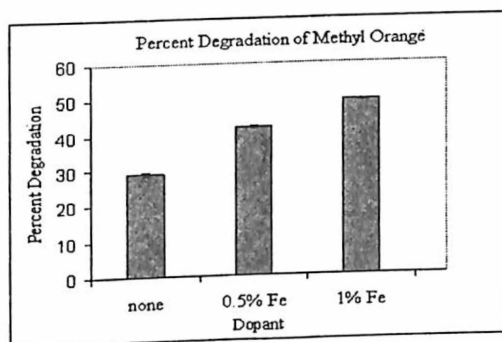
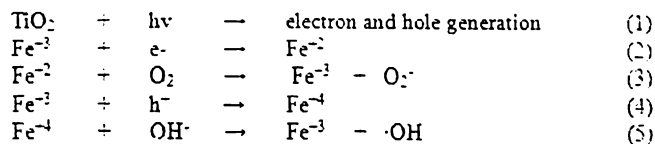


Figure 6. Percent Degradation of Methyl Orange with Doped and Undoped Titania Nanotubes

Undoped titania is expected to show poor photocatalytic behaviour under white light as titania's high band gap energy of 3.2 eV prevents photon absorption in the visible region. The almost 30% methyl orange degradation is actually surprisingly high as other researches points to much lower activity under white light [2,3,6]. This would probably due to the absence of a UV filter for the light source (150W metal halide) and high UV amounts may have been present. With the introduction of the metal ion, lower energy radiation is expected to be absorbed [22]. Furthermore, another benefit of adding dopant could be explained as follows. The small amount of Fe^{+3} can act as a temporary photo-generated electron or hole-trapping site and inhibits the recombination of photo-generated charge carriers and prolongs their lifetime [15]. The detailed reaction steps are as follows:



The formation of O_2^\cdot and $\cdot\text{OH}$ free radicals (steps 3 and 5) have an important implication. These free radicals are the species responsible for interacting and breaking down the organic substance into simple molecules [3]. It is also important to note that the photocatalytic activity of Fe-TiO₂ nanorods is strongly dependent on the dopant concentration since the Fe^{+3} ions can serve not only as a mediator of interfacial charge transfer but also as a recombination center [7].

Aside from the effect of doping, the combined effect of its fine crystallite structure leading to a high surface area would contribute to its high catalytic behaviour as this reaction is indeed surface area dependent [17]. Furthermore, the one-dimensional structure of nanotubes has the ability to enhance the transfer and transport of charge carriers [22]. By increasing the mobility of holes and electrons, the effective formation of free radicals that breaks down organic matter occurs with more frequency.

4. CONCLUSION

Titania nanotubes were successfully fabricated using the hydrothermal process. Fe(III)-doping was also carried out by a simple impregnation-calcination process. Transmission electron microscopy analysis revealed the nanotube structure in the samples while x-ray diffraction test confirmed the anatase form of titania. The surface area was observed to increase with increasing concentration of dopant. The Fe-doped samples also exhibited an enhanced photocatalytic property when operating under white light. The high photocatalytic activity of the Fe-doped TiO₂ powders could be attributed to the combined effects of Fe-doping, large specific surface area and small crystallite size. These fabricated doped nanotubes could now be used in future applications where its photocatalytic activity would be employed.

REFERENCES

1. H. Schmidt, "Nanoparticles by chemical synthesis, processing to materials and innovative applications", *Applied Organometallic Chemistry* 15 (2001) 331-343.
2. X. Chen, S.S. Mao, "Titanium dioxide nanomaterials: synthesis, properties, modifications, and applications", *Chemical Reviews* 107 (2007) 2891-2959.

3. Sakae Amemiya, "Titanium-Oxide Photocatalysts" Three bond Technical News, Tokyo, Japan Jan 1, 2004.
4. B.S. Bhatkhande, V.G. Pangarkar, A.A.C.M. Beenackers, "Photocatalytic degradation for environmental applications - a review", *Journal of Chemical Technologies: Biotechnology* 77 (2001) 102–116.
5. X. Fu, W.A. Zeltner, M.A. Anderson, "Applications in photocatalytic purification of air, in: P.V. Kamat, D. Meisel (Eds.), *Semiconductor Nanoclusters. Studies in Surface Science and Catalysis*, Elsevier Science, Amsterdam (1996) 445–461.
6. H. Langhuan, S. Zhongxin, L. Jiangliang, "N-doped TiO₂ Nanotubes with Visible-Light Photoactivity for Degradation of Methyl Orange" *Journal of the Ceramic Society of Japan* 115, 1 (2007) 28-31.
7. J.Yu, Q. Xiang, M. Zhou; "Preparation, characterization and visible-light-driven photocatalytic activity of Fe-doped titania nanorods and first-principles study for electronic structure", *Applied Catalysis B: Environmental* 90 (2009) 595–602.
8. J.C. Yu, Jianguo Yu, H. Wingkei, J. Zitao, and Z. Lizhi, "Effects of F⁻ Doping on the Photocatalytic Activity and Microstructures of Nanocrystalline TiO₂ Powders", *Chemistry of Materials* 14, 9 (2002) 3808–3816.
9. Y.F. Zhu, L. Zhang, L.Wang, Y. Fu, L.L. Gao, "The preparation and chemical structure of TiO₂ film photocatalysts supported on stainless steel substrates via the sol-gel method", *Journal of Materials Chemistry* 11 (2001) 1864–1868.
10. T. Leistner, K. Lehmbacher, P. Härter, C. Schmidt, A.J. Bauer, L. Frey, H. Ryssel, "MOCVD of titanium dioxide on the basis of new precursors", *Journal of Non-Crystalline Solids* 303 (2002) 64–68.
11. J. Wei, J. Yao, X. Zhang, W. Zhu, H. Wang and M.J. Rhodes, "Hydrothermal growth of titania nanostructures with tunable phase and shape", *Materials Letters* 61, 23-24 (2007) 4610-4613.
12. H. Sayilkan, "Improved photocatalytic activity of Sn⁺⁴-doped and undoped TiO₂ Thin film coated stainless steel under UV-and VIS-irradiation", *Applied Catalysis A: General* 319 (2007) 230–236.
13. S. Zhang, L.-M. Peng, Q. Chen, G. H. Du, G. Dawson, and W. Z. Zhou, "Formation Mechanism of H₂Ti₃O₇ Nanotubes", *Physical Review Letters* 91, 256103 (2003)
14. J. Yu, H. Yu., B. Cheng, "Effects of Calcination Temperature on the microstructure and photocatalytic activity of titanate nanotubes" *Journal of Molecular Catalysis A: Chemical* 249 (2006) 135-142
15. M. Zhou, J. Yu, B. Cheng, "Effects of Fe-doping on the photocatalytic activity of mesoporous TiO₂ powders prepared by sol-gel method" *Applied Catalysis A* 178 (1999) 191-203
16. F. Sayilkan, M. Asiltürk, P. Tatar, N. Kiraz, Ş. Şener, E. Arpaç and H. Sayilkan, "Photocatalytic performance of Sn-doped TiO₂ nanostructured thin films for photocatalytic degradation of malachite green dye under UV and VIS-lights", *Materials Research Bulletin* 43, 1 (2008) 127-134.
17. S. Kim, W. Choi, "Visible-light Induced Photocatalytic Degradation of 4-Chlorophenol and Phenolic Compounds in Aqueous Suspension of Pure Titania: Demonstrating the Existence of Surface-Complex-Mediated Path", *Journal of Physical Chemistry B* 109 (2005) 5143.
18. L. Shouxin, C. Xiaoyun, C. Xi, "Preparation of N-doped Visible-light Response Nanosize TiO₂ Photocatalyst Using the Acid-Catalyzed Hydrolysis Method", *Chinese Journal of Catalysis*. 27 (2006) 697-702.
19. H. Ou, S. Lo, "Review of Titania Nanotubes synthesized via the Hydrothermal Treatment: Fabrication, Modification and Application", *Separation and Purification Technology* 58 (2007) 179-191.
20. J. Yu, H. Yu, B. Cheng, M. Zhou, X. Zhao, "Enhanced photocatalytic activity of TiO_x powder (P25) by hydrothermal treatment", *Journal of Molecular Catalysis A: Chemical* 253 (2006) 112-118.
21. Y. Hsuan, H. Lin., C. Kuo, Y. Li, C. Huang, "Thermostability of Nano-TiO₂ and its Photocatalytic Activity", *Chemistry and Material Science* 89 (2006) 63-69.
22. U. Diebold, "The Surface Science of Titanium Dioxide", *Surface Science Reports* 48 (2003) 53-229.